

## Tests of integrated ceilings and the construction of simulation models

Zhilun Lyu<sup>\*1</sup>, Masakazu Sakaguchi<sup>2</sup>, Tomoharu Saruwatari<sup>3</sup> and Yasuyuki Nagano<sup>\*\*1</sup>

<sup>1</sup>Graduate School of Simulation Studies, University of Hyogo, 7-1-28 Minatojima-minamimachi, Chuo-ku, Kobe, Hyogo, Japan

<sup>2</sup>Asahibuilt Industry Corporation Limited, 4-32, Ota-ku, Tokyo, Japan

<sup>3</sup>JSOL Corporation, 2-2-4 Tosabori, Nishi-ku, Osaka, Japan

(Received November 29, 2018, Revised April 11, 2019, Accepted June 3, 2019)

**Abstract.** This paper proposes a new approach to model the screw joints of integrated ceilings via the finite element method (FEM). The simulation models consist of the beam elements. The screw joints used in the main bars and cross bars and in the W bars and cross bars are assumed to be rotation springs. The stiffness of the rotation springs is defined according to the technical standards proposed by the National Institute for Land and Infrastructure Management of Japan. By comparing the results of the shear tests and the simulation models, the effectiveness and efficiency of the simulation models proposed in this paper are verified. This paper indicates the possibility that the seismic performance of suspended ceilings can be confirmed directly via beam element models using FEM if the stiffnesses of the screw joints of the ceiling substrates are appropriately defined. Because cross-sectional shapes, physical properties, and other variables of the ceiling substrates can be easily changed in the models, it is expected that suspended ceiling manufactures will be able to design and confirm the seismic performance of suspended ceilings with different cross-sectional shapes or materials via computers, instead of spending large amounts of time and money on shake table tests.

**Keywords:** integrated ceiling; seismic ceiling; ceiling modules; FEM analysis

---

### 1. Introduction

#### 1.1 Mandatory earthquake resistance of suspended ceilings

In the great East Japan earthquake of March 11, 2011, collapses of suspended ceilings were observed in facilities 400 km from the epicenter. This earthquake prompted an amendment to the Enforcement Ordinance of Construction Standard Law (2013a) in 2013. In this revision, the earthquake resistance of suspended ceilings became mandatory. In the same year, the National Institute for Land and Infrastructure Management *et al.* (2013b) published the *Explanations of the Technical Standards for the Prevention of the Collapse of Ceilings in Buildings*. Technical

---

\*Corresponding author, Ph.D. Student, E-mail: [sb15v003@sim.u-hyogo.ac.jp](mailto:sb15v003@sim.u-hyogo.ac.jp)

\*\*Corresponding author, Professor, Dr. Eng., E-mail: [nagano@sim.u-hyogo.ac.jp](mailto:nagano@sim.u-hyogo.ac.jp)

standards for integrated ceilings have therefore been specified.

However, because the new standards only apply to new construction and refurbishments, a large number of suspended ceilings may still pose a danger. In the 2016 Kumamoto earthquake (National Institute for Land and Infrastructure Management *et al.* 2016a) and the 2018 Osaka earthquake (Cabinet Office, Government of Japan, 2018a), several collapses of suspended ceilings were reported. Suspended ceilings collapse not only during large earthquakes but also during normal periods. On July 14, 2018, parts of ceiling substrates in the Sendai Media Library collapsed and caused one injury (2018b). Therefore, even though their seismic performance is obligatory and the standards for suspended ceilings are being regulated, it is urgent to develop approaches to evaluate the seismic performance of existing and newly developed suspended ceilings.

### 1.2 Studies on integrated ceilings

In recent years, the number of studies on suspended ceilings has grown rapidly. Because ceiling panels are simply inserted into grids that are fabricated by ceiling substrates, the stiffnesses of integrated ceilings, a type of suspended ceiling, are considered to be low. Therefore, a large number of studies on suspended ceilings have focused on the performance of integrated ceilings.

Most previous studies on suspended ceilings, however, have primarily focused on experimental evaluations of suspended ceilings. In these studies, shake table tests have been used to confirm the seismic performance of suspended ceilings (e.g., Cosenza *et al.* 2015a; Wang *et al.* 2016b; Pourali *et al.* 2017a) and ceiling components (e.g., Soroushian *et al.* 2015b, c, d). Studies that focus on numerical analysis are rare.

Conversely, studies on structural members frequently use the finite element method (FEM) to confirm the seismic performance of the structural members. Di Sarno L *et al.* (2015e, 2017b) developed FEM models to predict the seismic response of the tested cabinets. The analytical result was closely matched with the experimental result until the cabinet exhibits the rocking mechanism. Mizushima *et al.* (2018c) created a detailed finite element (FE) model using the LS-DYNA software. Their paper shows that the behaviors of structural members can be analytically simulated with extremely high accuracy. In addition, Isobe *et al.* (2018d) attempted to develop a numerical code to analyze the motion of furniture, a type of nonstructural member, subjected to seismic excitations. Meanwhile, Manoj *et al.* (2018e) determined the response of orthotropic laminated composite plate using FEM. The results can be used into application such as aircrafts, rockets, etc.. It is believed that it can also be helpful to use FEM to evaluate the seismic performance of suspended ceilings during the design. It is expected that, similar to the models of structural members, the accuracy of FE models of suspended ceilings can be improved.

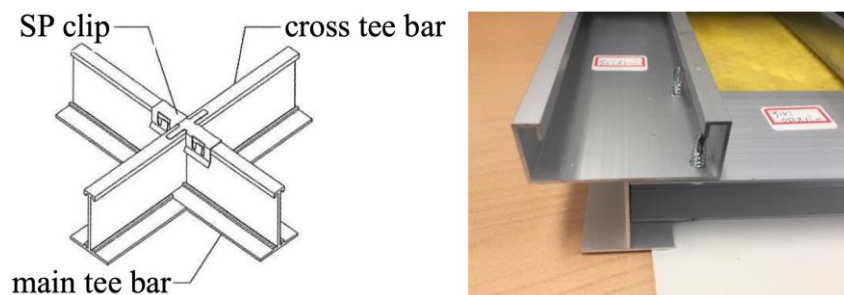


Fig. 1 Ceiling substrates used in conventional integrated ceilings (left) and in new integrated ceilings (right)

Sakaguchi (2018f), one of co-authors of this paper, developed a new construction method for lightweight integrated ceilings using V-shaped bracing members. Unlike the elements used in conventional integrated ceilings (e.g., main tees, cross tees, and C-channels), the ceiling substrates used in this new type of integrated ceiling are completely different in shape (Fig. 1). The details of these ceiling substrates are shown in Section 2.2.

### 1.3 Purpose

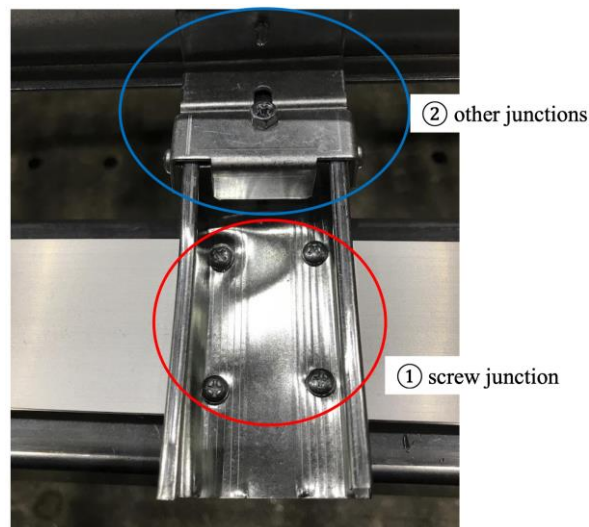


Fig. 2 Junctions of ceiling substrates

In this paper, we discuss shear tests on this new type of integrated ceiling and propose a new approach to simulate models of integrated ceilings. To confirm the in-plane stiffness of the ceiling surface, a shear test was conducted using a shaking table. Meanwhile, the in-plane stiffness was confirmed via a simulation model. As a preliminary study, a simulation model was created with the beam elements. It is thought that ceiling substrates may rotate at the screw junctions (Fig. 2); therefore, the screw junctions were modeled as rotation springs. Other junctions, for example, the one shown in Fig. 2, were treated as rigid bodies. The shear test and the simulation model are discussed in detail in Sections 2 and 3, respectively.

It is expected that the performance of integrated ceilings (at any scale) can be confirmed via simulation models, and therefore, integrated ceiling makers will be able to save time and money on research and development.

## 2. In-plane shear test of a ceiling module

### 2.1 Introduction

To confirm the hysteresis characteristics of the integrated ceiling and the states of the ceiling surface at several given loads, in-plane shear tests were conducted. The tests were conducted at the Research and Testing Center of the General Building Research Corporation of Japan.

2.2 Specimens

Fig. 3 shows one of the specimens 1000 × 1500-C, where 1000, 1500, and C stand for the intervals of the main bars, the intervals of the cross bars, and the cross bar (the loading direction), respectively. The ceiling substrates and their cross sections are shown in Fig. 4.

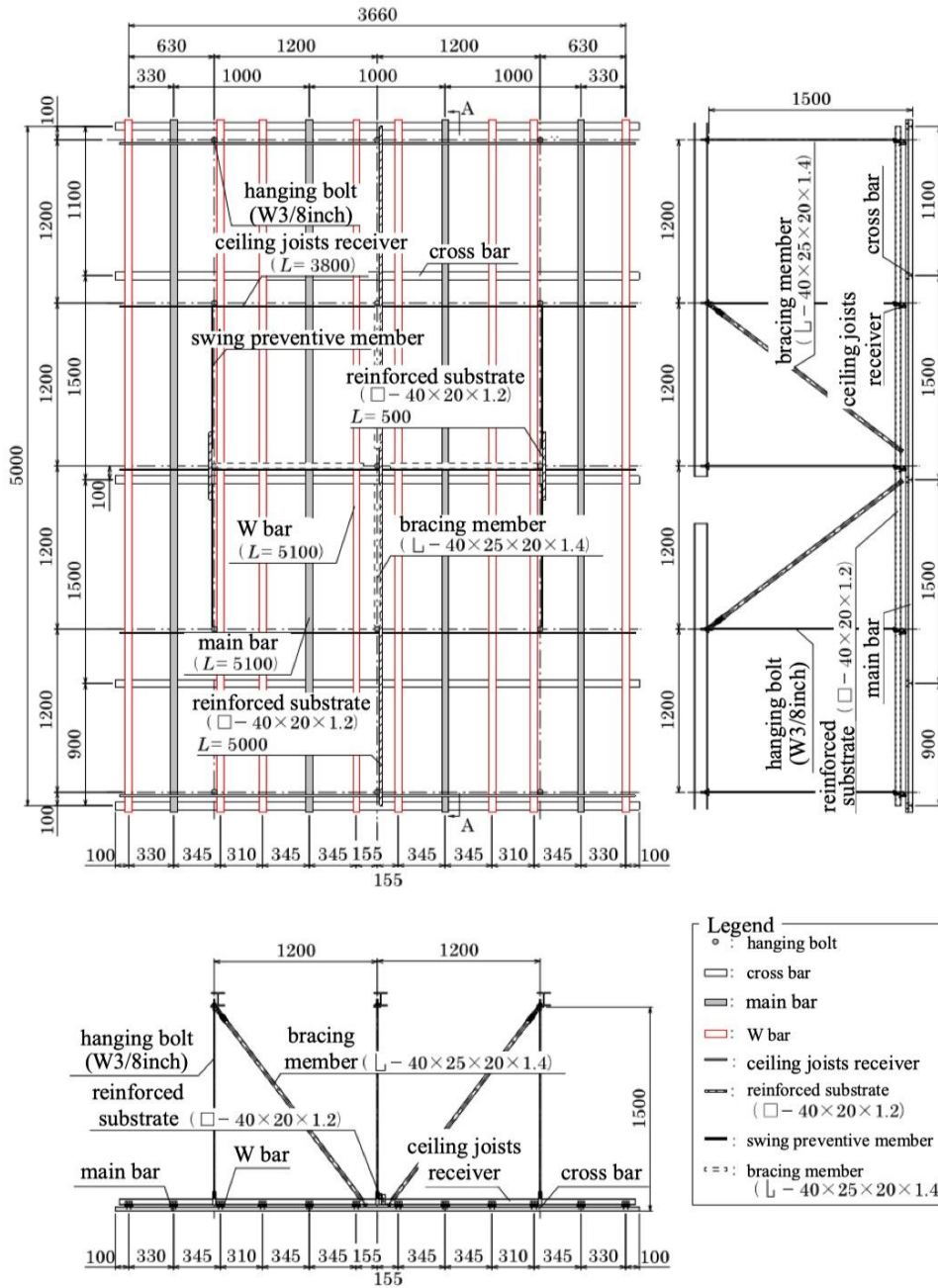


Fig. 3 Ceiling unit (1000 × 1500-C) (dimension: mm)

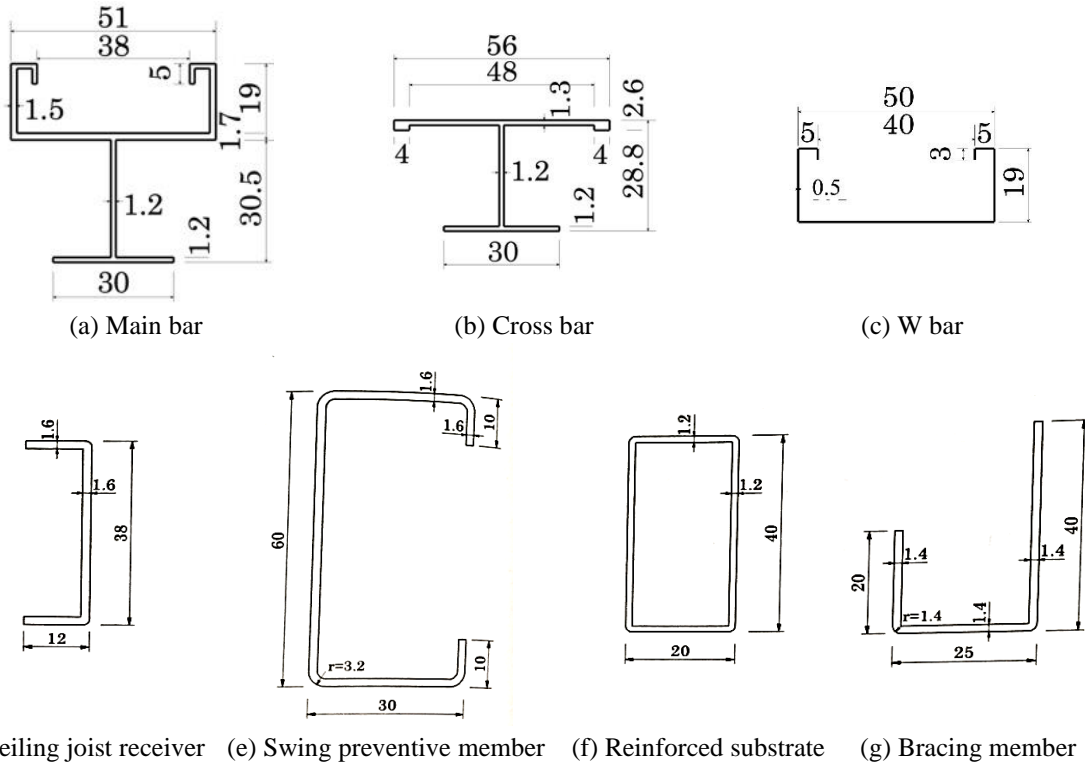


Fig. 4 Ceiling substrates of a suspended ceiling (dimension: mm)

### 2.3 Testing methods

Fig. 5 shows the apparatus for the in-plane shear tests. The forces were loaded horizontally at the edges of the ceiling surface via two hydraulic jacks. The displacements and loading directions were kept the same.

Fig. 6 shows the cycle of the loading forces. The forces were loaded at  $\pm 0.5 G$ ,  $\pm 1.3 G$ ,  $\pm 2.2 G$ , and  $\pm 3.3 G$  three times each, and then the loading was maintained continuously at the maximum stroke of the hydraulic jack, which is according to Explanations of the Technical Standards for the Prevention of the Collapse of Ceilings in Buildings (2013b). 0.5, 1.3 and 2.2 are horizontal seismic coefficients for the suspended ceilings at different floors, which are required in the Notification No.771 of Ministry of Land, Infrastructure, Transport and Tourism of Japan. 3.3, which is 1.5 times of 2.2, is used to confirm the seismic performance of suspended ceilings at inertia forces that beyond the requirement. The value 1.0 G is approximately 763 N and was calculated using the following steps.

$$w = A \times w_1 = 17.28 \text{ m}^2 \times 4.5 \text{ kg/m}^2 = 77.76 \text{ kg} \tag{1}$$

$$M = 77.76 \text{ kg} \times 9.807 \text{ N/kg} = 763 \text{ N} \tag{2}$$

Here,  $w$ ,  $A$ ,  $w_1$ , and  $M$  stand for the mass of the ceiling module, the area that one pair of bracing members bears, the average of the mass of the ceiling module in one square meter, and the weight of the ceiling module, respectively. Therefore,  $\pm 0.5 G$ ,  $\pm 1.3 G$ ,  $\pm 2.2 G$ , and  $\pm 3.3 G$  for this integrated ceiling correspond to  $\pm 382 \text{ N}$ ,  $\pm 992 \text{ N}$ ,  $\pm 1679 \text{ N}$ , and  $\pm 2518 \text{ N}$ , respectively.

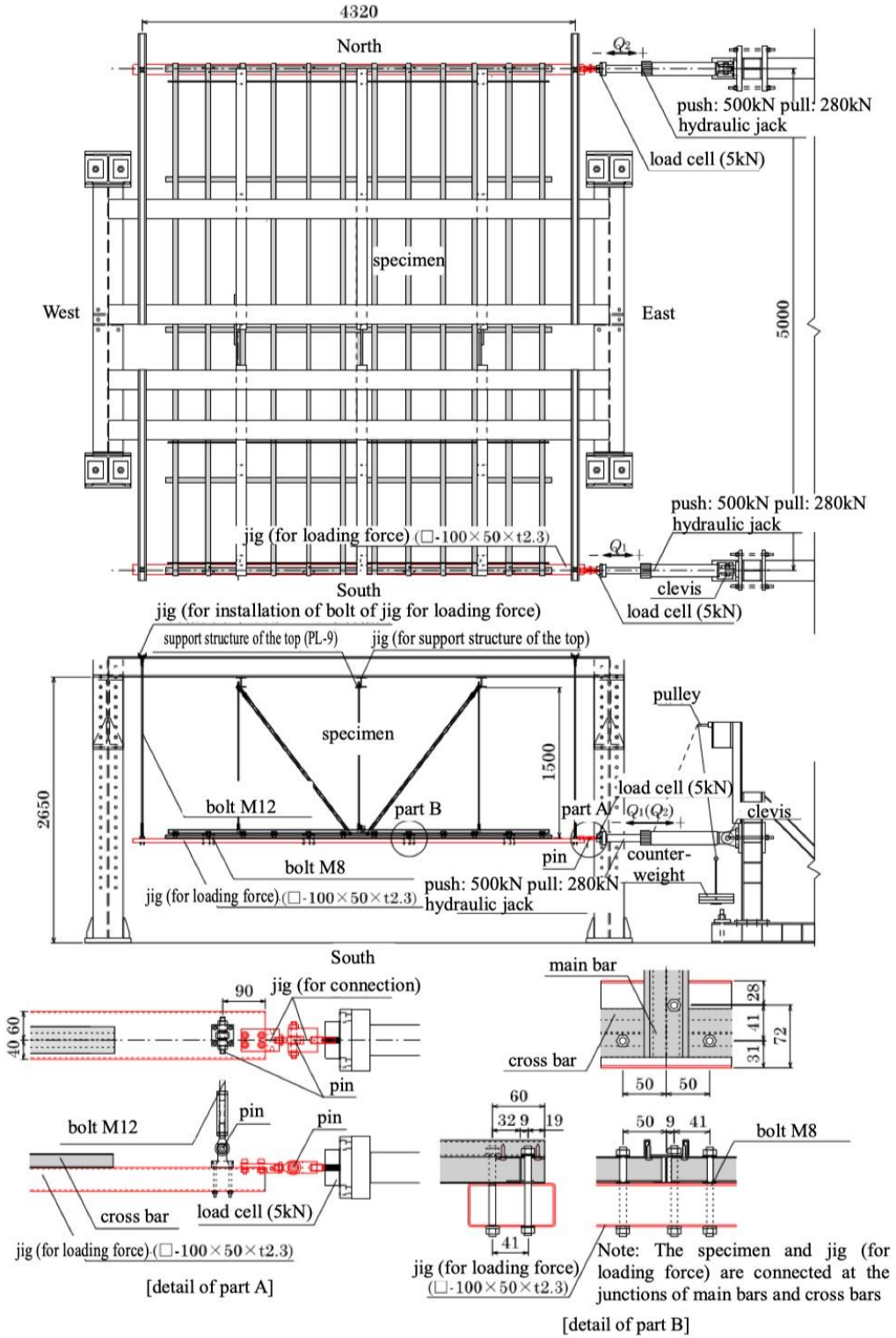


Fig. 5 Testing methods

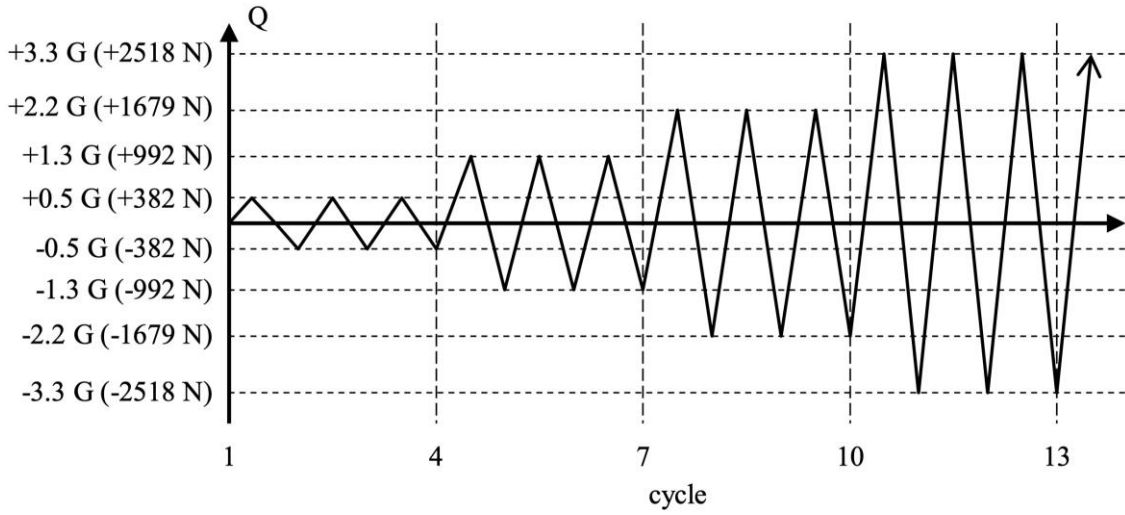


Fig. 6 Cycles of the loading forces

2.4 Test results

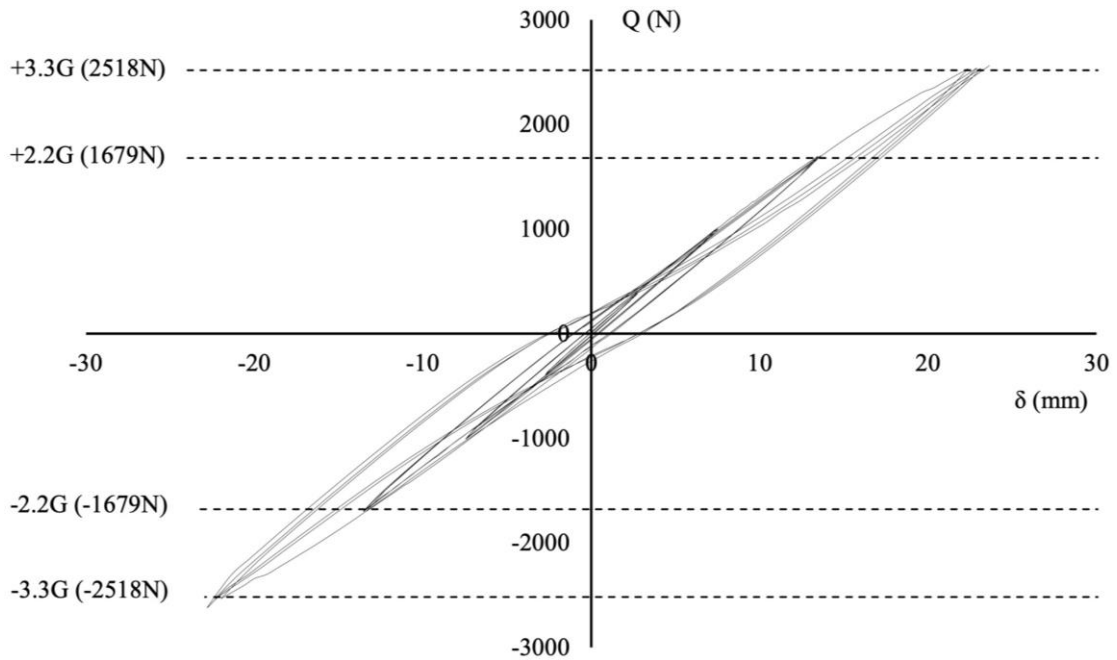


Fig. 7  $Q$ - $\delta$  relationship (by  $\pm 3.3$  G)

Figs 7 and 8 show the  $Q$ - $\delta$  relationships of the specimen  $1000 \times 1500$ -C.  $Q$  is the loading force of two hydraulic jacks, whereas  $\delta$  is the average displacement of two loading points. It can be confirmed that the ceiling surface is linear elastic for  $\pm 2.2$  G. The residual displacement is approximately 1.2 mm.

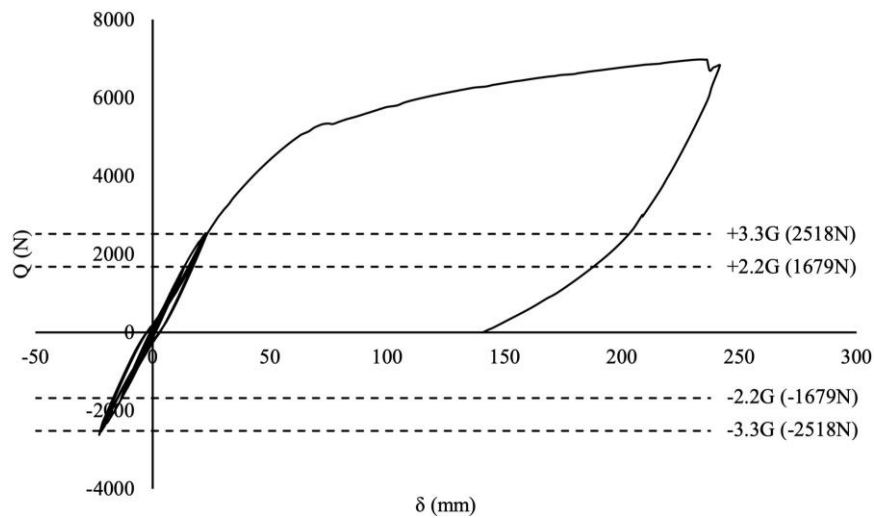


Fig. 8  $Q$ - $\delta$  relationship (for the maximum force)

### 3. Simulation models

#### 3.1 Introduction

In this section, the simulation model for the ceiling unit tests is introduced.

The pre- and post-processing of the simulation analysis were performed using the simulation modeling software program Jvision (ver. 3.4.0 (rev.13719), JSOL Corporation). The analysis of the simulation models was conducted using the FEM analysis software LS-DYNA (ver. R7.0.0, rev. 79055).

Fig. 9 shows the model of the specimen 1000  $\times$  1500-C, which is created based on the Fig. 3. The model consists of main bars, cross bars, W bars, ceiling joist receivers, swing preventive members, reinforced substrates, and bracing members. The numbers of nodes and elements are 7731 and 7678 (free nodes included), respectively. The analysis time for this model was approximately 1 h.

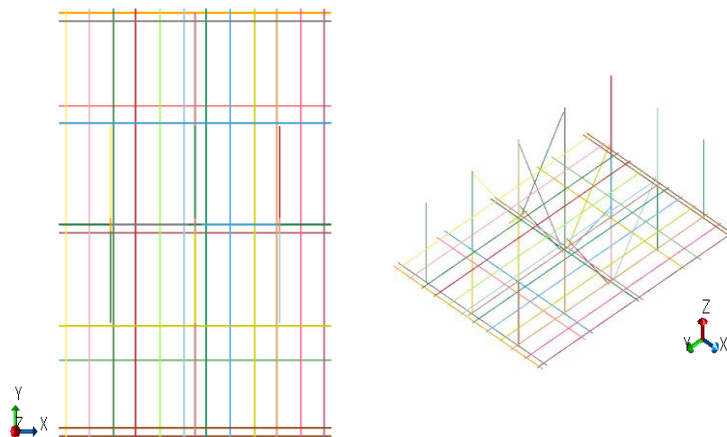


Fig. 9 Example of a simulation model (M450)



3.2 Cross sections and material properties of the ceiling substrates

Table 1 Areas and moment of inertia areas of the ceiling substrates

Ceiling substrates	Area (mm <sup>2</sup> )	I <sub>tt</sub> (mm <sup>4</sup> )	I <sub>ss</sub> (mm <sup>4</sup> )
W bar	50.5	2661.76	19,801.71
Cross bar	147.64	21,230.49	28,772.71
Main bar	230.88	53,931.29	62,374.80
Ceiling joist receiver	94.08	1087.20	18,347.03
Swing preventive member	213.76	27,108.16	122,207.37
Reinforced substrate	138.24	28,702.52	9584.44
Suspending bolt	71.33	404.89	404.89
Bracing member	115.08	15,983.12	6015.73

Table 2 Material properties

Member	Density (t/mm <sup>3</sup> )	Young's Modulus (N/mm <sup>2</sup> )	Poisson Ratio	Yield Stress (N/mm <sup>2</sup> )
Main bar	$2.7 \times 10^{-9}$	70000	0.33	176
Cross bar				161
W bar				
Ceiling joist receiver	$7.85 \times 10^{-9}$	$2.05 \times 10^5$	0.3	295
Swing preventive member				
Reinforced substrate				
Hanging bolt				
Bracing member				

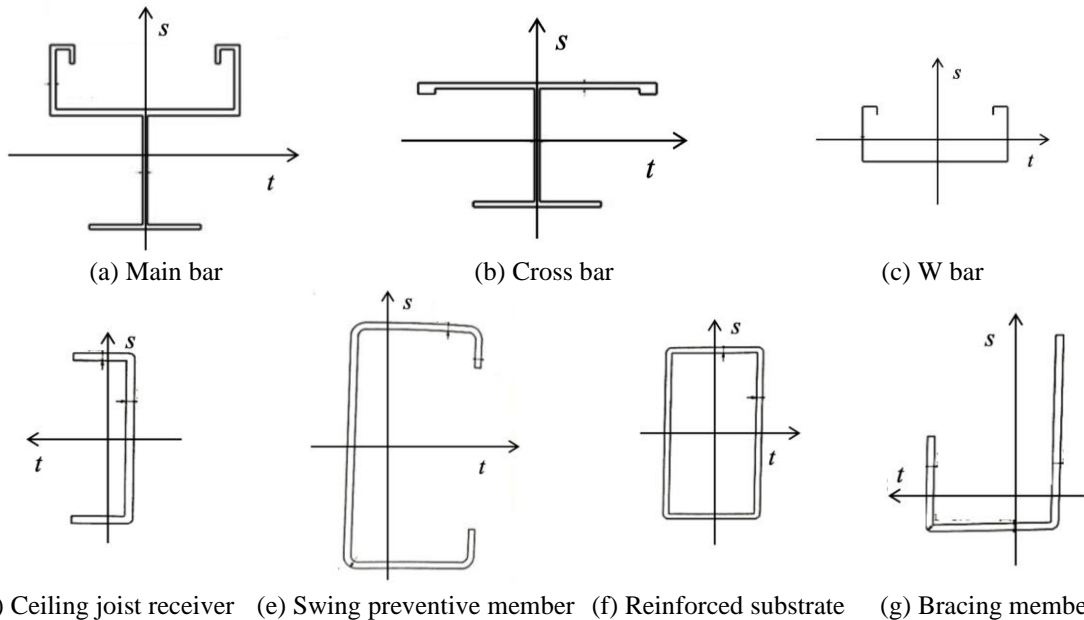


Fig. 10 Local coordinate system of each ceiling substrates

Fig. 4 depicts the cross sections of all the ceiling substrates used in the integrated ceiling, and Table 1 shows the areas and moment of inertia areas of the ceiling substrates.  $I_t$  is the moment of inertia area of the t axis, whereas  $I_{ss}$  is that of the s-axis. The t axis and s axis, together with the r axis, are the axes of the local coordinate system, which are used to determine the direction and properties of the beam elements in LS-DYNA. Fig. 10 shows the t-axis, s-axis, and r-axis of each ceiling substrate, which are defined according to the manual of Jvision.

Table 2 shows the material properties of the ceiling substrates. The main bars and cross bars are made of steel, whereas the other substrates are made of aluminum. The yield stresses of the main bars, W bars, and cross bars are determined on the basis of the material tests. Lacking experimental data of the other ceiling substrates, the yield stresses of such ceiling substrates are assumed to be the same as that of the W bars.

### 3.3 Boundary conditions

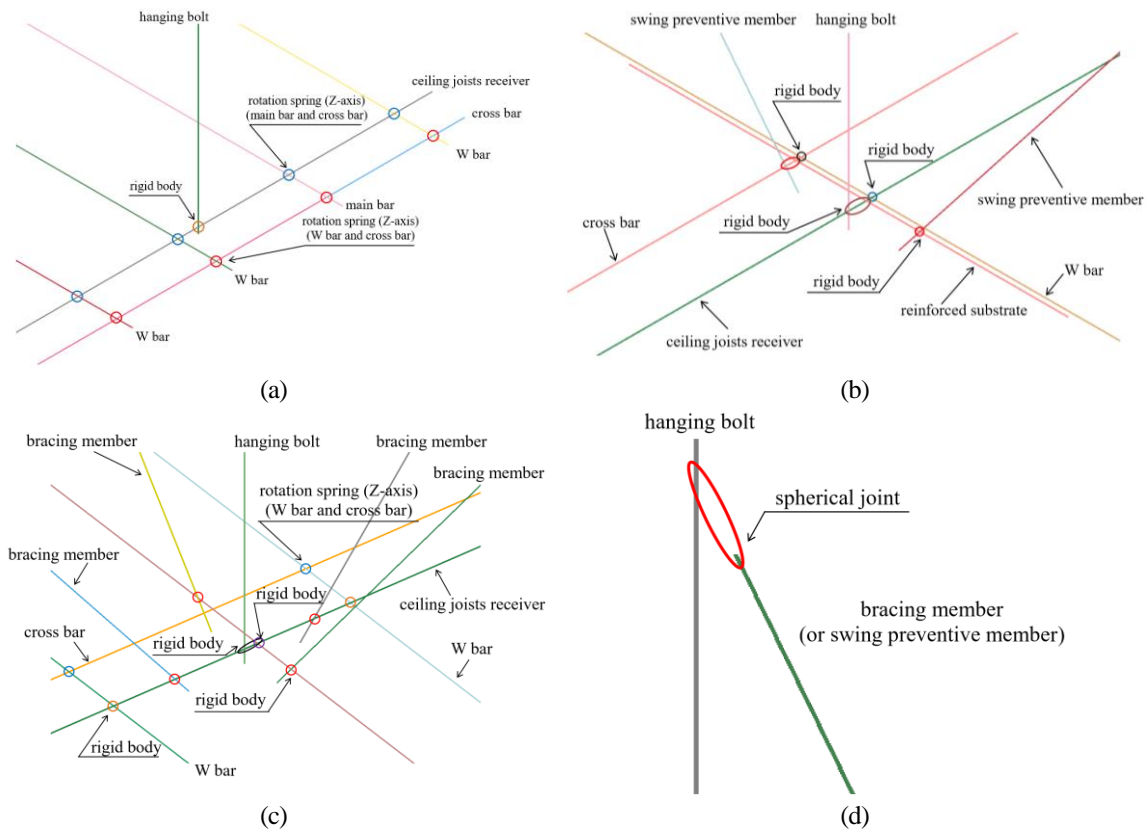


Fig. 11 Boundary conditions

Fig. 11 depicts the boundary conditions of the simulation model. Junctions between the following parts are set to be nodal rigid bodies (Figs. 11(a)–(c)).

- Ceiling joist receivers and W bars
- Ceiling joist receivers and main bars
- Ceiling joist receivers and reinforced substrates

- Ceiling joist receivers and hanging bolts
- Reinforced substrates and swing preventive members
- Bracing members and reinforced substrates
- Bracing members and ceiling joist receivers

The tops of the bracing members (or the swing preventive members) are connected to the adjacent hanging bolts via spherical joints (Fig. 11(d)).

The transition and rotation of nodes at the tops of all hanging bolts are constrained.

### 3.4. Rotation springs of screw joints

Screw joints of main bars and cross bars, W bars and cross bars are assumed to be rotation springs in the simulation model. The stiffnesses of screw joints are defined according to the results of cross-section tests of ceiling substrates and calculated according to the technical standards.

Fig. 12 shows the testing method of cross-section tests of ceiling substrates. Fig. 13 shows the moment – rotation relationships of the junctions of each specimen. Moment  $M$  and Rotation  $R$  are calculated by Eqs. (3) and (4)

$$M = 2PH \tag{3}$$

$$R = \delta / (2H) \tag{4}$$

$P$ ,  $H$ ,  $\delta$  infer to the force at the loading point, the length of cross bar, and the displacement of loading point, respectively.

Table 3 shows the  $M_d$ ,  $M_a$ , and  $K_d$  of each specimen.  $M_d$ ,  $M_a$ ,  $K_d$  stands for moment at equivalent damaged point, moment at equivalent allowable load (2/3 of  $M_d$ ), and initial stiffness, respectively.

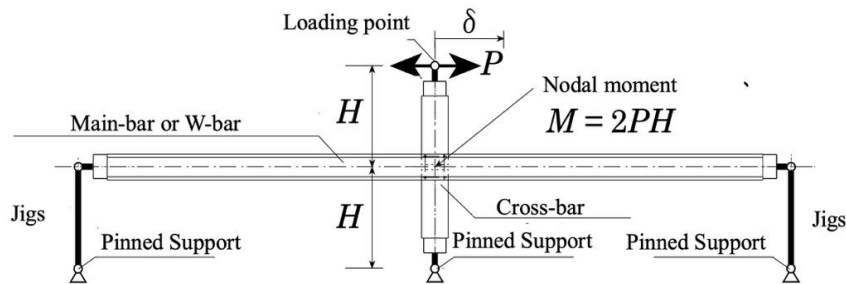


Fig. 12 Testing methods

Table 3 List of the combinations and results of the tests

Combination	L (mm)	H (mm)	$M_d$ (Nm)	$M_a$ (Nm)	$K_d$ (Nm/(10 <sup>-3</sup> rad))
M750-U	750	200	91		6.89
M500-U	500	250	92	Ave. 61	8.29
M450-U	450	300	92		7.80
W750-D	750	200	100		11.0
W500-D	500	250	93	Ave. 63	12.7
W450-D	450	300	94		12.2

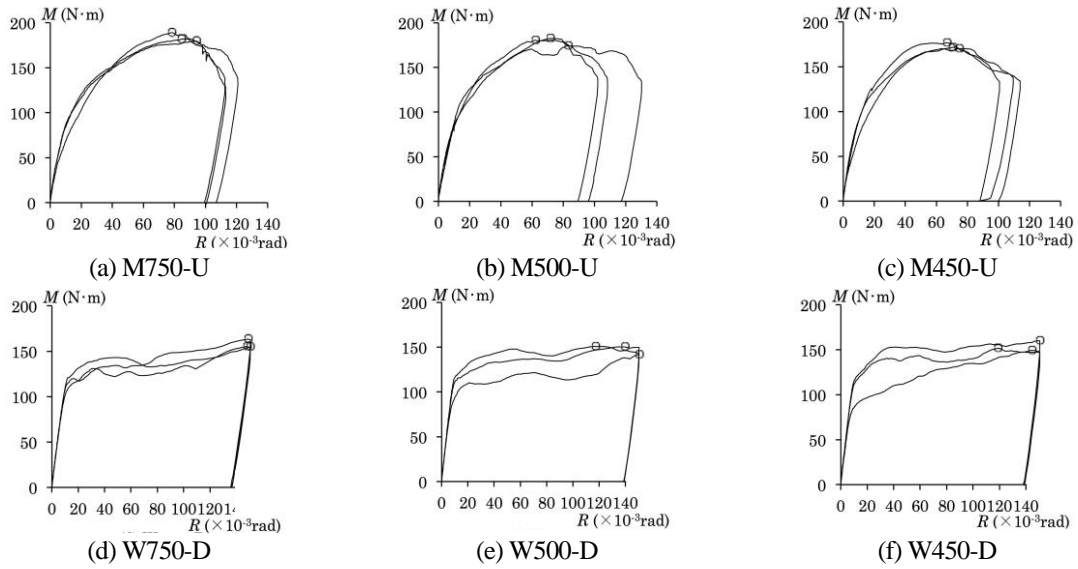


Fig. 13 M-R relationships (monotonic loading tests)

The stiffness of rotation spring defines according the following steps.

1) The initial stiffness of  $K$  of rotation spring defines according to the test result. According to the table 3, the initial stiffness of rotation springs of main bars and cross bars are defined as 10,000 Nm/rad. On the other hand, the stiffnesses of W bars and cross bars are well corresponded to the tests when the connections are defined as rigidities by the trials and errors. Therefore, the initial stiffness of rotation springs of W bars and cross bars are defined as 100,000 Nm/rad, which is 10 times of that of main bars and cross bars.

2) The first break point is determined according to the moment at equivalent allowable load (60 Nm). Because specimen M750-U (or M500-U, M450-U) consists of 2 cross bars and 1 main bar, there are 2 rotation springs in the model. Thereby, the first break of rotation springs of main bars and cross bars is set half of the moment at equivalent allowable load.

3) Other break points are determined according the test results (Fig. 12).

Fig. 14 shows the stiffnesses of rotation springs of main bar and cross bar, W bar and cross bar.

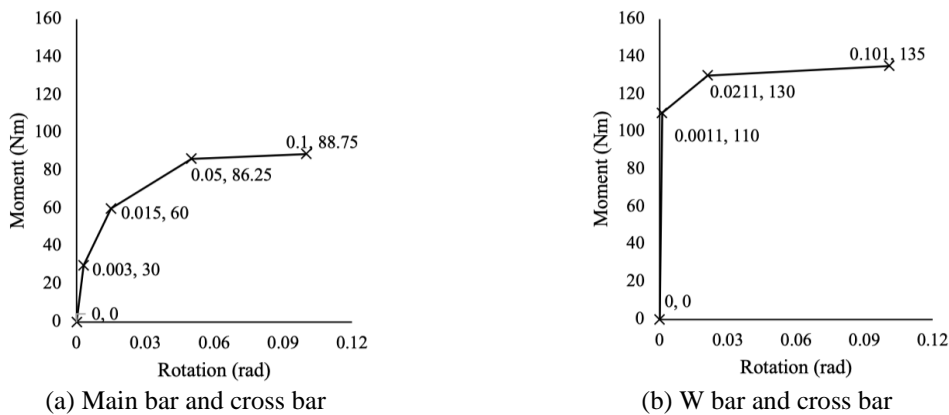


Fig. 14 Stiffness of the rotation springs

### 3.5. Simulation results

Fig. 15 shows a comparison of the  $Q$ – $\delta$  relationships for the shear test (black line) and the simulation model (red line).  $Q$  is the total of the loading forces at the two loading nodes, whereas  $\delta$  is the displacement of the loading nodes (either). The initial stiffness (by 5 mm) of the simulation model is about 211.12 N/mm, while that of the shear test is about 137.95 N/mm. The initial stiffness of the ceiling model is approximately 1.53 times stiffer than that of the test result. Fig. 16 shows the deformation (displacement scale: 5.0) of the simulation model from four different views at a displacement of 50 mm.

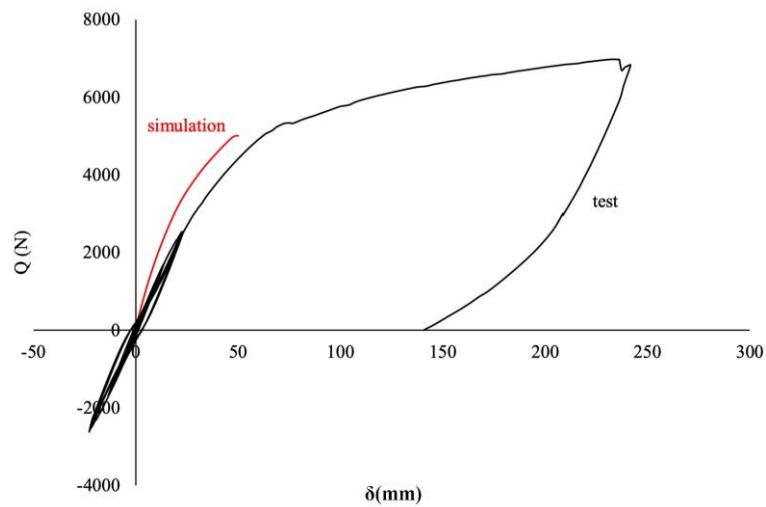


Fig. 15 Comparisons of the displacement–load relationships of the simulations and the tests

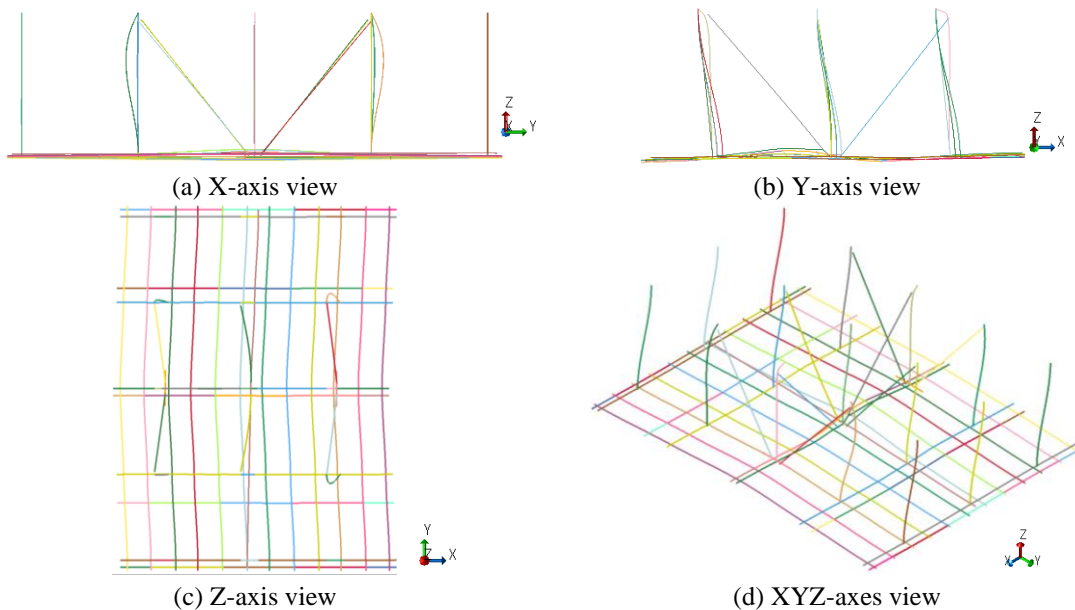


Fig. 16 Deformation of the ceiling model (displacement scale: 5.0)

### **3.6 Discussion**

The initial stiffness of the ceiling model is larger than that of the shear tests. The reason for this is thought to be that the models of the other junctions of the ceiling substrates are simply set to be nodal rigid bodies and are not defined according to the actual material properties. However, due to the lack of experimental data for these junctions, the actual material properties remain to be determined in the future studies. In addition, the stiffness of the rotation springs needs to be directly defined via simulations of ceiling substrates in future studies.

## **4. Conclusions**

In this paper, we proposed a new approach to model the screw joints of integrated ceilings based on shear tests. The ceiling substrates and the construction of the integrated ceilings are completely different from those of conventional integrated ceilings. Therefore, we proposed a new method to model these integrated ceilings. In our method, a simulation model is created using the beam elements. The screw joints used in the main bars and cross bars and in the W bars and cross bars are assumed to be rotation springs; the stiffnesses of which are defined according to the results of shear tests and the technical standards. Meanwhile, the other junctions are assumed to be nodal rigid bodies.

The deformation of this new type of integrated ceiling is confirmed in the simulation model. Though the initial of simulation model is about 1.53 times larger than that of the shear test, which results from this study demonstrates the possibility of confirming the seismic performance of integrated ceilings via simulation models, if the properties of other junctions are confirmed and well modeled.

Traditionally, the seismic performance of suspended ceilings has been confirmed via shake table tests. However, shake table tests are costly and their maximum input acceleration is limited. In addition, the specifications of suspended ceilings cannot be changed while the shake table tests are being conducted, unless the shake tables are owned by the suspended ceiling manufacturer. The use of simulation models, however, can solve these problems. The cross-sectional shapes, physical properties, and other variables of the ceiling substrates can be easily changed, and it is expected that suspended ceiling manufacturers will be able to design and confirm the seismic performance of suspended ceilings with different cross-sectional shapes or materials at any scale via computers, instead of spending large amounts of time and money on shake table tests. Moreover, the maximum input acceleration is not limited in FEM, and the seismic performance can be confirmed with any seismic wave using the simulation models proposed in this paper.

## **Acknowledgments**

The in-panel shear test is conducted at General Building Research Corporation of Japan. During the test, we received a lot of constructional advices from Director Nobuyuki Yasui. The study on simulation models of integrated ceilings is financially supported by the Japanese Society of Steel Construction (JSSC). We would like to express our deepest appreciation to Director Nobuyuki Yasui and the JSSC for their support.

## References

- ATS Suspended Ceiling (2018f), Asahi Built Industry Corporation, Tokyo, Japan. [http://www.a-bl.co.jp/publics/index/58/&anchor\\_link=page58](http://www.a-bl.co.jp/publics/index/58/&anchor_link=page58).
- Cabinet Office (2018a), About damage states in earthquake in the northern Osaka, Government of Japan, Japan. [http://www.bousai.go.jp/updates/h30jishin\\_osaka/pdf/300625\\_jishin\\_osaka\\_02.pdf](http://www.bousai.go.jp/updates/h30jishin_osaka/pdf/300625_jishin_osaka_02.pdf).
- Cosenza, E., Di Sarno, L., Maddaloni, G., Magliulo, G., Petrone, C. and Prota, A. (2015a), “Shake table tests for the seismic fragility evaluation of hospital rooms”, *Earthq. Eng. Struct. Dyn.*, **44**(1), 23-40. <https://doi.org/10.1002/eqe.2456>.
- Di Sarno, L., Petrone, C., Magliulo, G. and Manfredi, G. (2015e), “Dynamic response analysis of typical medical components”, *Eng. Struct.*, **100**(1), 442-454. <https://doi.org/10.1016/j.engstruct.2015.06.036>.
- Ministry of Construction of Japan (2013a), Enforcement Ordinance of the Building Standard Law, Article 39, Ministry of Construction, Japan.
- Isobe, D., Yamashita, T., Tagawa, H., Kaneko, M., Takahashi, T. and Motoyui, S. (2018d), “Motion analysis of furniture under seismic excitation using the finite element method”, *Japan Architectural Review*, **1**(1), 44-55. <https://doi.org/10.3130/aijs.80.1891>.
- Manoj, N., Achintya, C. and Avadesh, K.S. (2018e), “Harmonic analysis of moderately thick symmetric cross-ply laminated composite plate using FEM”, *Adv. Comput. Design*, **3**(2), 113-132. <http://dx.doi.org/10.12989/acd.2018.3.2.113>.
- Mizushima, Y., Mukai, Y., Namba, H., Taga, K. and Saruwatari, T. (2018c), “Super-detailed FEM simulations for full-scale steel structure with fatal rupture at joints between members—Shaking-table test of full-scale steel frame structure to estimate influence of cumulative damage by multiple strong motion: Part 1”, *Japan Architectural Review*, **1**(1), 96-108. <http://dx.doi.org/10.3130/aijs.81.61>.
- National Research and Development Agency Japan, Building Research Institute (2016a), “The 14<sup>th</sup> investigation on building damages in Kumamoto earthquake”, <https://www.kenken.go.jp/japanese/contents/topics/2016/14-kumamoto.pdf>.
- National Institute for Land and Infrastructure Management (2013b), “Explanations of the technical standards for the prevention of the collapse of the ceilings in the buildings”, Japan.
- Petrone, C., Di Sarno, L., Magliulo, G. and Cosenza, E. (2017b), “Numerical modelling of typical hospital building contents”, *Bullet. Earthq. Eng.*, **15**(4), 1609-1633. <https://doi.org/10.1007/s10518-016-0034-1>.
- Pourali, A., Dhakal, R.P., MacRae, G. and Tasligedik, A.S. (2017a), “Fully floating suspended ceiling system: Experimental evaluation of structural feasibility and challenges”, *Earthq. Spectra*, **33**(4), 1627-1654. <https://doi.org/10.1193/092916EQS163M>.
- Sendai City Official Website (2018b), [https://www.city.sendai.jp/kikakune/180714\\_rinjikyukan.html](https://www.city.sendai.jp/kikakune/180714_rinjikyukan.html).
- Soroushian, S., Maragakis, E.M. and Jenkins, C. (2015b), “Capacity evaluation of suspended ceiling components, part 1: experimental studies”, *J Earthq. Eng.*, **19**(5), 784-804. <https://doi.org/10.1080/13632469.2014.998354>.
- Soroushian, S., Maragakis, E.M. and Jenkins, C. (2015c), “Capacity evaluation of suspended ceiling components, part 2: analytical studies”, *J Earthq. Eng.*, **19**(5), 805-821. <https://doi.org/10.1080/13632469.2015.1006345>.
- Soroushian, S., Maragakis, E.M., Ryan, K.L., Sato, E., Sasaki, T., Okazaki, T. and Mosqueda, G. (2015d), “Seismic simulation of an integrated ceiling-partition wall-piping system at E-Defense. II: Evaluation of nonstructural damage and fragilities”, *Japan Architectural Review*, **142**(2), [https://doi.org/10.1061/\(ASCE\)ST.1943-541X.0001385](https://doi.org/10.1061/(ASCE)ST.1943-541X.0001385).
- Wang, D., Dai, J., Qu, Z. and Ning, X. (2016b), “Shake table tests of suspended ceilings to simulate the observed damage in the Ms 7.0 Lushan earthquake, China”, *Earthq. Eng. Eng. Vib.*, **15**(2), 239-249. <https://doi.org/10.1061/10.1007/s11803-016-0319-z>.